Investigation of domain walls in periodically poled MgO:$LiNbO_3$ by second harmonic imaging

Yunlin Chen (陈云琳)*, Jinhong Zhang (张进宏), and Haiwei Li (李海伟)

School of Science, Beijing Jiaotong University, Beijing 100044, China

**Corresponding author: ylchen@bjtu.edu.cn*

Received September 12, 2012; accepted November 16, 2012; posted online February 28, 2013

The domain wall regions in periodically poled MgO-doped $LiNbO_3$ (PPMgLN) crystal are examined by using second harmonic generation (SHG). The results show that the average domain walls that separate the individual domains have a width in the order of about 1 μm, and the walls are neither completely smooth nor uniform along the walls from the imaging of the SHG. It is proposed that the origin of the second harmonic signal in the regions around domain wall is attributed to the non-180° domain walls in the ferroelectric domains.

OCIS codes: 160.2100, 190.2620.

doi: 10.3788/COL201311.031601.

Ferroelectric single crystals are composed of domains, with each domain having a uniform spontaneous polarization. The transition regions of opposite spontaneous polarization are called domain walls. Domain engineering for producing desired ferroelectric domain structures with precise parameters in the ferroelectric single crystals has become more mature, especially for the most often used periodically poled ferroelectrics materials, such as $LiNbO_3$(PPLN), $LiTaO_3$ (PPLT), and $KTiOPO_4$ (PPKTP). Electric field-induced 180° anti-parallel ferroelectric domains are separated by boundaries of infinitely narrow and parallel domain walls. The ferroelec-tric behavior is commonly explained by the rotation of domains and domain walls that are present in the crystal with uniform polarization[1−3]. A lot of work has been done on domain wall and estimation of its width, the width of the domain walls has been very controversial, with many authors claiming that the walls are very wide. Recently, Bandyopadhyay *et al.*[4] have studied the domain wall and its width control the ferroelectric behavior. Direct observations of ferroelectric domains are routinely performed by using linear optical polarization microscopy. A second harmonic generation (SHG) technique has been recently developed to visualize various ferroelectric, ferromagnetic, and multiferroic domain structures[5,6] that relies on the interference between the second harmonic (SH) waves generated from various domains.

In this letter, we investigated in detail the induced second harmonic generation from the ferroelectric domain walls in high-quality PPMgLN. In contrast to the other known nondestructive methods[7−9], this technique allows to measure not only the domain sizes and domain inversion duty-cycle ratio, but also the domain wall parameters. From the experimental results we can draw the conclusion that the SH signal in the regions around a domain wall is attributed to the non-180° domain walls in the ferroelectric domains.

In our experiment we used several z-cut MgO:LN wafer with dimensions of 15×10×1 (mm), which were polished down to a thickness of 0.5 mm, and anti-parallel 180° domains were then fabricated using the electric field poling technique at room temperature[10]. The ferroelectric domain inversion period of the sample is 20 μm. The schematic diagram of the experimental setup for probing the domain microstructure and domain walls is illustrated in Fig.1. The fundamental laser beam is from a mode-locked Ti: sapphire laser with a high repetition rate of 82 MHz at the wavelength of 810 nm. The laser pulse has a temporal width of about 100 fs. This fundamental laser beam is then focused onto the sample, which is mounted on a translation stage, by a long focus lens to achieve a spot size of approximately 139 μm in radius. This results in the incidence peak intensity of about 40 MW/cm^2 at the sample position. The SH wave generated in the crystal passes through a 50×micro-objective (numerical aperture, NA=0.55) and is detected by a charge-coupled device (CCD) connected to a computer. A half-wave plate is mounted on the rotating stepper motors to adjust the polarization directions of the fundamental laser beam. The laser is polarized parallel to the sample's y axis, and the x-polarized SH is detected.

The transmitted SH waves from the domain walls can be observed clearly. Figure 2 shows the image of the SH intensity from the sample with the period 20 μm. The walls appear as bright strips. The bright stripes of the SHG variation correspond exactly to the ferroelectric domain length, and the largest variation of the SHG intensity is observed in the areas around domain walls. The bright stripes have an average width of about 1 μm and vary for different domain walls along the x axis of the sample. Figure 3 shows the normalized SH

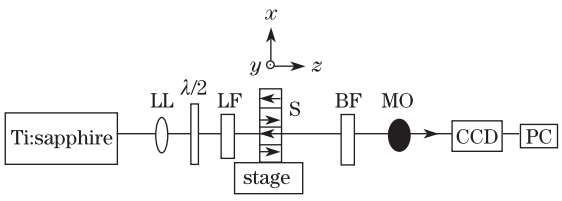

Fig. 1. Schematic of the SHG through a PPMgO:LN crystal along its z axis. LL: long-focus lens; LF: long-pass filter; BF: bandpass interference filter; MO: micro-objective; $\lambda/2$: half-wave plate; CCD: charge-coupled device; PC: computer; S: sample.

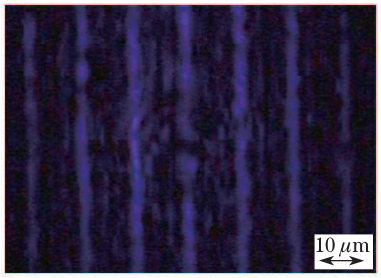

Fig. 2. SH imaging of PPMgLN crystal with the period of 20 μm.

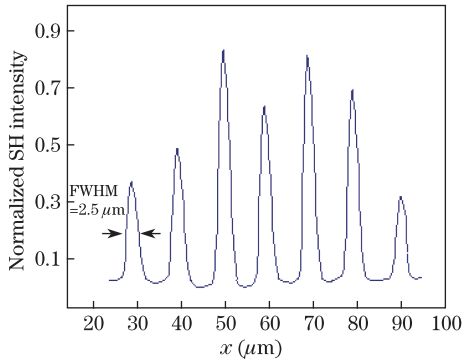

Fig. 3. SH intensity measured at room temperature for the crystal's position along the x axis.

intensity along the sample's x axis. The full-width at half-maximum (FWHM) is about 2.5 μm, which shows that the nonlinearity enhancement occurs within 2.5 μm around the ferroelectric domain walls.

When taking into account the convolution of the illumination with the domain walls during the imaging this suggests a maximum wall thickness of about 1 μm, which is as same as the result of Ref. [11]. One may note from the Fig. 2 that the strips run in a slight zigzag across the imaged areas and that the domains within a period of the crystal are almost equally wide. From Figs. 2 and 3 a duty cycle (the ratio of the domain width to the period) can be estimated to be 0.5.

Figure 4 shows the scanning electron microscope (SEM) image of the sample following 5 minutes etching. The SEM images shown here suggest that the maximum width of the reversal domain wall is almost 1 μm and the duty cycle is about 0.5 within an overall 20-μm period for this sample. Indeed, the domain wall patterns are asymmetric as shown in Fig. 4, and the image indicates that the spread of the domain reversal differs between the two directions of poling. This might be the main reason for the induced variations in the brightness of SHG along the domain walls.

In fact, anti-parallel domains are equivalent with respect to linear optical properties and even with respect to nonlinear intensity characteristics. We measured the dependence of the SH power generated in the domain wall regions as a function of the fundamental beam polarization as shown in Fig. 5. The generated SH light power depends only on the fundamental wave polarization and is independent from the periodical domain inversion structure. In contrast to this observation for the PPMgO:LN sample, single-domain MgO:LN crystals do not produce any observable SH light using the same process.

The origin of the observed SH generated at domain wall regions has not yet been clarified. Some explanations have been proposed to explain the origin of SH generated at the domain wall regions in KTP. In KTP crystal, the SH imaging of the domain wall has been attributed to the microscatterers in the domain wall regions[12]. In order to explain the second order nonlinear response in the domain walls of PPKTP, it was proposed that the strain fields in these regions caused a DC piezoelectric field[13]. It is thought that the random distribution of light-emitting centers in the domain walls may be excited by the pump wave to radiate at the SH frequency[14].

Here we attribute the SH generated at the domain wall regions due to non-180° domain walls generated by pinning defects of the domain wall. These pinning defects are thought to be physical defects such as screw dislocations or localized variations of point defects[15]. During the poling process, the pinning points will change in curvature of the domain wall around them. Such bending of the domain walls around pinning defects has been predicted in ferroelectric materials[16]. Because of the pinning defects of the domain wall, there is a divergence of polarization across the walls. A 180° wall at an angle to the c axis would have an associated electric field normal to the wall of $\sim (P_s/\varepsilon\varepsilon_0)\cos^2(90\text{-}\theta)$. Such non-180° domain walls in ferroelectric domain wall regions can be observed by pyroelectric field imaging. These non-180° domain walls can give rise to structural anisotropy of the domain walls,

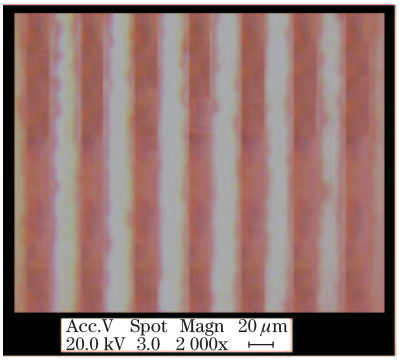

Fig. 4. SEM patterns of PPMgLN after 5-min etching at 90 °C.

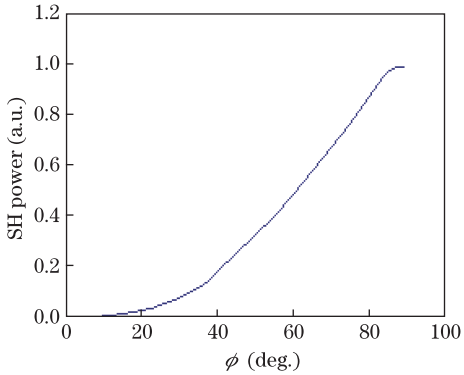

Fig. 5. SH power versus the fundamental beam polarization.

which can be modeled by a random distribution of light-emitting centers (excited by the pump wave to radiate at the SH frequency), superimposed to a single domain MgO:LN crystal do not generate a SH signal. Therefore, we can conclude that such non-180° domain walls can contribute significantly to the SHG within the domain wall regions.

In conclusion, using SH signals we visualize 180° domain walls in PPMgLN crystals. Our results show that the domain walls that separating the individual domains have an average width in the order of about 1 μm, and that the walls are neither completely smooth nor uniform along the walls determined from the SH imaging. Imaging from SH signals can be used as a powerful and simple technique to characterize the domain inversion properties, such as domain size, domain inversion duty-cycle ratio, and the domain wall thickness in the PPMgLN. The origin of the SH signal in the regions around domain wall is attributed to the non-180° domain walls caused by the domain inversion process.

This work was supported by the National Natural Science Foundation of China (No. 61178052) and the Fundamental Research Funds for the Central Universities (Nos. 2011JBZ013 and 2011JBM122).

References

1. S. Kim, V. Gopalan, and A. Gruverman, Appl. Phys. Lett. **80,** 2740 (2002).
2. D. A. Scrymgeour, V. Gopalan, A. Itagi, A. Saxena, and P. J. Swart, Phys. Rev. B **71,** 184110 (2005).
3. A. K. Bandyopadhyay and P. C. Ray, J. Appl. Phys. **95,** 226 (2004).
4. A. Bandyopadhyay, A. Sengupta, K. Choudhary, A. K. Bandyopadhyay, and P. C. Ray, World J. Condensed Matter Phys. **2,** 91 (2012).
5. Bas B. Van Aken, J. Rivera, H. Schmid, and M. Fiebig, Nature **449,** 702 (2007).
6. Y. Zhang, F. Wang, K. Geren, S. N. Zhu, and M. Xiao, Opt. Lett. **35,** 178 (2010).
7. S. MacCormack and J. Feinberg, Appl. Opt. **35,** 5961 (1996).
8. V. Grubsky, S. MacCormack, and J. Feinberg, Opt. Lett. **21,** 6 (1996).
9. M. Müller, C. Langrock, E. Soergel, K. Buse, and M. M. Fejer, J. Appl. Phys. **97,** 044102 (2005).
10. Y. L. Chen, W. G. Yan, D. D. Wang, S. L. Chen, and G. Y. Zhang, Appl. Phys. Lett. **90,** 062908 (2007).
11. R. Brooks, P. D. Townsend, D. E. Hole, D. Callejo, V. Bermúdez, and E. Diéguez, J. Phys. D: Appl. Phys. **36,** 969 (2003).
12. B. Vohnsen and B. I. Bozhevolnyi, J. Microscopy **202,** 244 (2001).
13. A. Fragemann, V. Pasiskevicius, and F. Laurell, Appl. Phys. Lett. **85,** 375 (2004).
14. M. Flörsheimer, R. Paschotta, U. Kubitscheck, Ch. Brillert, D. Hofmann, L. Heuer, G. Schrei-ber, C. Verbeek, W. Sohler, and H. Fuchs, Appl. Phys. B **67,** 59 (1998).
15. T. J. Yang, U. Mohiaeen, and M. C. Gupta, Appl. Phys. Lett. **71,** 1960 (1997).
16. E. K. H. Salje and Y. Ishibashi, J. Phys. Condens. Matter **8,** 8477 (1996).